

1 **Blue mussels *Mytilus edulis* L. and *M. trossulus* Gould in sympatry: assessment of ecological niche**
2 **divergence using species distribution modeling**

3 **Running page head: “*Mussel species niche divergence*”**

4 V. Khaitov^{*1,2}, P. Safonov³, A. Zaichikova⁴, M. Katolikova¹, M. Ivanov¹, P. Strelkov^{1,5}

5 ¹ St. Petersburg State University, University embankment 7–9, 199034 St. Petersburg, Russia

6 ² Kandalaksha State Nature Reserve, Lineynaya 35, 184042 Kandalaksha, Russia

7 ³ Institute of Cytology RAS, Tikhoretsky 4, 194064 St. Petersburg, Russia

8 ⁴ Moscow State University, Leninskie gory 1c12, 119234 Moscow, Russia

9 ⁵ Laboratory of Monitoring and Conservation of Natural Arctic Ecosystems, Murmansk Arctic
10 University, Kapitana Egorova 15, 183038 Murmansk, Russia

11 * Corresponding author

12 Corresponding author's e-mail: polydora@rambler.ru

13 *Abstract*

14 Species distribution models (SDMs) describing the relationship between species occurrence and
15 environmental parameters can be used to assess the ecological niche of a species. Usually applied to
16 morphologically distinct species, SDMs are also a promising tool for describing niche partitioning in
17 coexisting cryptic species. An example of the latter in the marine realm are blue mussels *Mytilus edulis*
18 (*ME*) and *M. trossulus* (*MT*). Despite considerable research effort, little is known about how they share
19 space and resources in sympatry anywhere except the Baltic Sea. Salinity, substrate, surf and proximity
20 to harbors have been suggested as candidate factors of segregation but no general consensus has been

21 reached. Here we assessed partial effects of these predictors on divergence of *ME* and *MT* in the White
22 Sea littoral applying SDMs to 570 mussel samples with known taxonomic structure. We found that
23 each of the predictors influenced spatial segregation. The most expected habitat of *ME* was a bottom
24 substrate in a wind-exposed location with an average White Sea salinity (24 psu) away from ports and
25 large rivers, while for *MT* it was an algal substrate in a wind-protected area with a lower salinity close
26 to ports and large rivers. We also found that the species segregation by substrate was density-
27 dependent: the degree of segregation positively depended on *ME* abundance, which indicates that *ME*
28 outcompetes *MT* on bottom substrates. We suggest that the same predictors can drive the segregation of
29 these two species outside the White Sea.

30 Key words: *Mytilus*; cryptic species; species distribution models; ecological niche divergence

32 *1. INTRODUCTION*

33 Species distribution models (SDMs) are a numerical tool describing the relationship between species
34 occurrence and environmental parameters. They can be used to predict distribution patterns of species
35 in space and time and to assess their ecological niche (Elith & Leathwick 2009). Joint application of
36 SDMs to coexisting species, i.e. a community, makes it possible to describe the partitioning of their
37 ecological niches (Ovaskainen & Abrego 2020). In other words, SDMs may describe the axes in
38 ecological space along which coexisting species are segregated. SDMs can be built using various
39 approaches, from regular multiple regressions to advanced machine learning (Elith et al. 2006,
40 Caradima et al. 2019, Poggiato et al. 2021).

41 SDMs are usually applied to morphologically distinct species (e.g. Reiss et al. 2011, Lindegren et al.
42 2022), which are distinguished in routine biodiversity assessment studies. However, there is increasing
43 evidence about coexistence of cryptic species (Bickford et al. 2007, Geller et al. 2010, Struck et al.
44 2018) and infraspecific taxa (Dufresnes et al. 2023). ~~Cryptic invasions usually stand behind sympatry~~
45 ~~(Morais & Reichard 2017).~~ Sympatry usually arises as a result of cryptic invasions (Morais &
46 Reichard 2017). Coexisting taxa are unlikely to have identical ecological phenotypes, and an ecological
47 niche partitioning between them can be expected (Sáez & Lozano 2005). The question how such taxa
48 share space and resources in sympatry can be answered using SDMs (Peterson et al. 2019). This
49 approach has already been successfully used in marine ecology (e.g. Dennis & Hellberg 2010, Lowen
50 et al. 2019, Hu et al. 2021). The results indicate that cryptic taxa indeed have distinct ecological
51 phenotypes. Therefore, ecological niche assessment of coexisting cryptic species, particularly those of
52 economic, conservation or ecosystem importance, is a promising research direction.

53 Blue mussels (*Mytilus edulis* species complex) are the longest-known and best-studied cryptic species
54 in the marine realm (Knowlton 1993, Gosling 2021). Six species that make up this complex hybridize
55 in sympatry and are easier to distinguish genetically than morphologically (Wenne et al. 2020, Gardner
56 et al. 2021). Blue mussels are powerful ecosystem engineers and important aquaculture objects species
57 for aquaculture (Buschbaum et al. 2009, Gosling 2021).

58 The dominant species of blue mussels in the North Atlantic are *M. edulis* (*ME*) and *M. trossulus* (*MT*).
59 Their distribution on the oceanic scale is mostly regulated by temperature and its correlates such as sea
60 ice extent and primary production (Hayhurst & Rawson 2009, Wenne et al. 2020). Both of these
61 species occur in the Arctic but *ME* is distributed further south than *MT* in temperate seas (Wenne et al.
62 2020). There are multiple zones of sympatry between *ME* and *MT* (hereafter, contact zones), from
63 Scotland and the Gulf of Maine in the south to Greenland and Spitsbergen in the north (Wenne et al.
64 2020). *ME* and *MT* evolved in allopatry since the Pliocene in the Atlantic and the Pacific Ocean,
65 respectively, and their contact zones are thought to have formed as a result of repeated *MT* invasions
66 from the Pacific Ocean to the Atlantic as well as from one part of the Atlantic into another (Väinölä &
67 Strelkov 2011, Wenne et al. 2020 and references therein).

68 In contact zones, *ME*, *MT* and their hybrids are often found in the same settlements (Väinölä &
69 Strelkov 2011, Wenne et al. 2020), which are referred to as mixed settlements. Scientists generally
70 agree that sympatric *ME* and *MT* are ecologically distinct (Riginos & Cunningham 2005, Katolikova et
71 al. 2016, Michalek et al. 2021) and have a different economic value in aquaculture (Penney et al. 2002,
72 Beaumont et al. 2008), but the data on the factors of their ecological segregation are fragmentary and
73 contradictory.

74 The greatest progress in comparative ecological studies of *ME* and *MT* in sympatry has been made in
75 the contact zones in the Baltic Sea, in the waters of the Kola Peninsula (White and Barents Seas) and in
76 the West Atlantic (mainly, Gulf of Maine and ~~New Seotland~~ Nova Scotia). In the Baltic Sea, the
77 brackish areas of its inner part are inhabited by *MT*, while the saltier areas closer to the North Sea are
78 inhabited by *ME*. In the middle there is the contact zone, where mixed settlements can be dominated by
79 hybrids, with *MT* gene frequency gradually increasing towards the inner Baltic (Väinölä & Strelkov
80 2011, Zbawicka et al. 2014, Stuckas et al. 2017). As a result, the species distribution is strongly
81 correlated with salinity, and the role of other factors is negligible (Kijewski et al. 2019).

82 In the contact zones of the Kola Peninsula and the West Atlantic there are few hybrids in mixed
83 settlements, and the spatial distribution of *ME* and *MT* is patchy on different scales, from dozens of
84 kilometers to dozens of centimeters. The relationship between the distribution and salinity is not
85 obvious in these contact zones, and there seems to be no simple “single-factor” pattern driver of species
86 distribution (Riginos & Cunningham 2005, Katolikova et al. 2016, Wenne et al. 2020, Marchenko et al.
87 2023). Depth, fouling substrate, anthropogenic pollution levels and surf effects have been considered,
88 apart from salinity, as possible factors affecting the segregation of *ME* and *MT* (Bates & Innes 1995,
89 Comesaña et al. 1999, Hellou & Law 2003, Tam & Scrosati 2014, Marchenko et al. 2023) but no
90 consensus has been reached.

91 In particular, in the White and the Barents Sea, the frequency of *MT* is greater in port areas, possibly
92 because this species has been introduced into the region with ship traffic in historic times (Väinölä &
93 Strelkov 2011, Katolikova et al. 2016). The only segregation factor explicitly tested in the White Sea is
94 the substrate of littoral mussels (Katolikova et al. 2016). Adult *MT* is more common on fucoid algae
95 while adult *ME* mostly lives directly on the bottom substrates such as mud, sand, stones and gravel.
96 However, segregation across substrates cannot fully explain the local-scale patchiness (Katolikova et

97 al. 2016). In the Barents Sea, no correlation with substrate has been found. However, these species
98 have different depth preferences there: *ME* appears to be a more sublittoral species and *MT* a more
99 littoral one (Marchenko et al. 2023).

100 It should be noted that some of the candidate factors of species segregation may be collinear and
101 confound the analysis. Ports are often located in sheltered areas close to river mouths, and the effects of
102 shipping, surf and salinity are difficult to distinguish. The effects of depth and substrate may obscure
103 each other since fucoids, common in the littoral, are rare in the sublittoral, where they are replaced by
104 kelps (Druehl & Green 1982).

105 Comparative ecological studies of *ME* and *MT*, which began as early as the 1980s (see Riginos &
106 Cunningham 2005 for review), have been hampered by two circumstances. Firstly, it was impossible to
107 examine large amounts of material because species identification required labor-intensive genotyping
108 methods (Khaitov et al., 2021). Secondly, until recently there were no reliable statistical methods for
109 modeling the distribution of sympatric taxa in the space of multiple factors and the SDM approach
110 could not be implemented. To our knowledge, it has been applied to *ME* and *MT* only twice, in the
111 above-mentioned studies by Kijewski et al. (2019) and Wenne et al. (2020). In both studies the
112 machine learning techniques were used to model the macro-geographic distribution of species
113 (technically, of allele frequencies at taxonomically informative genes) in the space of multiple climatic
114 and oceanographic characteristics available from public databases. These methods have never been
115 applied to modeling species distributions within contact zones.

116 In our previous studies we found a simple semi-diagnostic **conchological** trait for *ME* and *MT*
117 (Katolikova et al. 2016). Using this trait, one could make reliable interpretations of the taxonomic

118 structure of mixed settlements on the basis of morphotype frequencies in samples, i.e., without
119 genotyping. This procedure was referred to as the “morphotype test” (Khaitov et al. 2021).

120 The aim of this study was to estimate the divergence of ecological niches between *ME* and *MT* in the
121 White Sea littoral along environmental gradients such as substrate, salinity, surf level, and distance
122 from ports. All these factors have been suggested as potentially influencing segregation of these two
123 species in sympatry. Another candidate factor, depth (Marchenko et al. 2023), was not examined in our
124 study but was controlled by sampling at the same littoral level. To achieve our aim, we examined the
125 variability of the environmental predictors and the taxonomic structure of mussel settlements using an
126 extensive material (95 study sites, 570 mussel samples, 55,529 mussels) and assessed the partial
127 influence of the predictors on the distribution of proportion of *MT* using SDMs. Since all predictors
128 were included in one model, collinearity could be controlled. Ideally, a model trained on reliable data
129 should be transferable and work well on independent data. Therefore, we evaluated the predictive
130 power of our model using testing datasets from the White and the Barents Sea. In addition, to reveal a
131 possible competition between the two species, we checked whether the pattern of their segregation by
132 substrate was density-dependent.

133 2. MATERIALS & METHODS

134 2.1 Study area

135 The study area was the Kandalaksha Bay, where all previous *ME* and *MT* studies in the White Sea have
136 been conducted (Katolikova et al. 2016, Khaitov et al. 2018, Khaitov et al. 2023). The Bay, 185 km
137 long, is funnel-shaped, with a highly indented coastline and numerous islands and skerries (Fig. 1).
138 Climate is continental subarctic with 4-5 months of ice cover and the average monthly sea surface
139 temperature in August of 13.8°C. Mean tidal range is about 2 m. Summer surface salinity is 24 psu in

140 most of the Bay (average salinity for the White Sea) and lower in the estuarine areas (Berger &
141 Naumov 2000). Two canals of a hydropower plant and 24 rivers with a catchment area of 141 – 12,830
142 km² (Median 240 km²; see **Table S1 in Supplement 1**) flow into the Bay, with the largest river, the
143 Niva, entering the Bay at its very top. Due to the indented shoreline and numerous rivers, local surf and
144 salinity gradients are pronounced (Filatov et al. 2007).

145 Six ports operating oceanic vessels were functioning in the area in the 20th century (**Fig. 1**). Two of
146 them, both at the Bay's top, are still in operation. The other four have been abandoned (Sailing
147 directions of the White Sea 1932, Krasavtsev 2011) but are occasionally visited by small ships (our
148 observations).

149 In 2002–2013, both *ME* and *MT* were almost ubiquitous in the Bay, but their ratio in settlements varied
150 greatly, with *ME* being generally dominant (Katolikova et al. 2016). Mussels in the Bay are particularly
151 abundant in the littoral furoid belt (mainly *Fucus vesiculosus* L. and *Ascophyllum nodosum* L.), which
152 is continuous 0.5-1.0 m above mean spring tide depth (Berger et al. 2001).

153 **2.2 Modeling dataset**

154 **2.2.1 Mussel sampling and processing**

155 Mussels were sampled at 95 sites within the littoral furoid belt in summer months of 2011-2018 (**Fig.**
156 **1**). Data for 17 of these sites were included in the study by Katolikova et al. (2016), the other data are
157 new (**Table S2 in Supplement 1**). The sites were chosen to describe the littoral populations of the Bay
158 in as much detail as possible and to account for the heterogeneity of their habitat by substrate type, surf
159 level, and distance from rivers and ports. All samples were taken within the furoid belt. At each site,
160 three samples from furoid thalli (hereinafter, algal samples) and three samples from bottom substrates
161 (bottom samples) were collected a few meters from each other using 0.25 m² and 0.025 m² frames,

162 respectively. A greater size of the algal frame was associated with the large size of the fucoids and the
163 need to account for their complex geometry. The frames were placed not randomly but approximately
164 at the same depth and in such a way as to capture the dense mussel aggregations.

165 We used mussels with a shell length larger than 10 mm for a reliable identification of the shell
166 morphotypes (Khaitov et al. 2021). In the bottom samples all mussels from a frame were used. In the
167 algal samples the procedure was different. One bundle of algae, containing at least a few dozen
168 mussels, was chosen and weighed together with the attached mussels. The rest of the algae from a
169 frame were weighted too. Mussels from the bundle were counted and used for further analysis. The
170 ratio between the counted number of mussels and the bundle weight was applied to the total algal
171 weight to reconstruct the total number of mussels in the sample (**Table S3 in Supplement 1**). The
172 information on the total number of mussels in algal samples was lacking for 12 of the sites, and they
173 were excluded from the analyses which required data on mussel abundance (**Model 2** and **Model 3**
174 below).

175 Mussel shell morphotypes were identified for all selected mussels as in Khaitov et al. (2021) based on
176 the presence (T-morphotype) or absence (E-morphotype) of an uninterrupted strip of prismatic layer
177 under the ligament on the inner side of the shell. T-morphotype is characteristic of *MT*, and E-
178 morphotype is characteristic of *ME*. The proportion of morphotypes was converted to the proportion of
179 *MT* (P_{tros}) in each sample, in pooled samples from each substrate from each site (**denoted as** $P_{tros_{Algae}}$
180 and $P_{tros_{Bottom}}$) and in pooled samples from each site ($P_{tros_{Site}}$), using equation

$$181 \quad P_{tros} = \frac{e^{-2.4+5.4PT}}{1 + e^{-2.4+5.4PT}}$$

182 where PT is a proportion of T-morphotype.

183

184 This equation, derived from the 24 genotyped samples (in total, 1105 multilocus mussel genotypes)
185 from the Kandalaksha Bay, accounts for the nearly linear dependence of *Ptros* on *PT* and reliably
186 predicts *Ptros* over the entire salinity range in the White Sea, i.e., up to 24 psu (Khaitov et al. 2021).
187 However, as studies in the Barents Sea have shown, this equation may overestimate *Ptros* at higher
188 salinities, e.g. up to 20% at salinity around 30 psu (Khaitov et al. 2021, Marchenko et al. 2023).

189 2.2.2 Assessment of environmental parameters

190 In total, we used seven parameters describing possible influence of rivers, ports, surf and substrate on
191 mussels (**Table 1**). We used three different proxies of salinity (*RiverSize*, *DistRiver* and *Salinity*)
192 because, ~~in our opinion~~, a single estimate of salinity at low tide could be insufficient to characterize
193 overall salinity and river influence per se at the sampling sites. *Salinity* was measured directly with an
194 accuracy of 1 psu using an Atago S/Mill-E refractometer. To classify rivers by size (*RiverSize*), the data
195 from ESM (**Table S1** in **Supplement 1**) were used. To calculate *Fetch*, the R-package “waver”
196 (Marchand & Gill 2018) was applied to regional ~~geographic map~~ shape-files.

197 2.3 Testing datasets

198 Three datasets were used as testing ones, one from the same area of the White Sea and two from the
199 Barents Sea. “Kandalaksha littoral” dataset contained 23 samples from 12 littoral sites in the
200 Kandalaksha Bay (**Fig. S1** in **Supplement 2**). We took only algal samples at four sites, only bottom
201 samples at four other sites and samples from both substrates at the remaining four sites (**Table S4** in
202 **Supplement 1**). Environmental parameters were assessed in the same way as for the modeling dataset.

203 “Tyuva littoral” and “Tyuva sublittoral” testing datasets were extracted from the published data of
204 Marchenko et al. (2023). These authors mapped in detail the distribution of *Ptros* in mussel settlements

of the 3-km-long Tyuva Inlet in the Kola Bay of the Barents Sea (**Fig. 1**) sampled in 2009-2010. *Ptros* was predicted either by direct genotyping or from morphotype frequencies using the formula derived for local populations existing under salinities higher than in the White Sea (Marchenko et al. 2023). They provided a number of environmental characteristics including depth, *Salinity*, cover of macrophytes in rank scale, and dominant algal species (usually, kelps in the sublittoral and fucoids on the littoral) for each sampling site. “Tyuva littoral” set contained samples from all 23 littoral sites from the depth range corresponding to the fucoid belt (0.5-1.5 m above mean spring tidal depth, Marchenko et al. [2023]; note that the position of fucoid belt in the Barents Sea differs from that in the White Sea due to the different tidal amplitude). “Tyuva sublittoral” contained samples from all 15 sublittoral sites (depth range from -0.5 to -3.5 m). Since the substrate of mussel fouling was not registered during sampling, we classified samples into bottom and algal ones by the algal cover in the sites (ranks 1-3 and 4-5, correspondingly). The remaining environmental parameters were assessed as for the modeling dataset, with the nearest port in Ekaterininskaya Gavan Bight considered as active and the river Tyuva flowing into the inlet as a large one.

2.4 Statistical analysis

All the data were processed using the statistical programming language R 4.05 (R Core Team 2023).

2.4.1 Dependency of *Ptros* on environmental parameters in modeling dataset (Model 1)

We used generalized additive mixed model (GAMM, Wood 2017) as a modeling technique, which has been shown to work well for SDM construction (Elith et al. 2006). One of the strengths of this approach is that additive models assume that the relationship between the dependent variable (in our case, *Ptros*) and continuous predictors is not necessarily linear but may be curvilinear (Austin 2002).

226 The weakness of the approach is that it does not provide a direct assessment of either relative or
227 absolute importance of factors.

228 GAMM fitted (hereafter, **Model 1**) was based on beta-binomial residuals distribution and the restricted
229 maximum likelihood method for estimation of the parameters. Smoothers for all continuous predictors
230 were fitted using cubic basic splines. Categorical predictors were included as parametric terms in the
231 model. Site was considered as a random factor. The function `gam()` from the package “mgcv” (Wood
232 2017) was used to fit the model.

233 To check for all predictors’ collinearity in **Model 1** and other models, we calculated the variance
234 inflation factor (VIF, Fox & Monette 1992), considering the value less than 3.5 as acceptable (Quinn &
235 Keough 2002). To verify that **Model 1** met the assumptions of sampling independence, we examined
236 the presence of residuals’ spatial autocorrelation by means of spline correlogram construction
237 (Bjørnstad & Falck 2001) with the function `spline.correlog()` from the package “ncf” (Bjornstad 2022)
238 and found no evidence of spatial autocorrelation. We also considered the model residuals in relation to
239 year of sampling and found no significant patterns.

240 **2.4.2 Dependence of abundance of mussels of different morphotypes on environmental** 241 **parameters in a modeling dataset (Model 2)**

242 The relationships between the taxonomic structure and the predictors were further investigated using
243 abundances of mussels of different morphotypes. This means that we equated morphotypes with
244 species. However, this assumption should not have crucially biased the results of the analysis, given the
245 proportional relationship between *PT* and *Ptros* in mussel settlements in the study area (Khaitov et al.
246 2021). The mean abundances of mussels of E- and T-morphotypes across samples from each site (from
247 both substrates) were log-transformed and used as the dependent variable in **Model 2**. The model was

constructed as a generalized additive one (GAM) with Gaussian residuals' distribution and included the factor *Morphotype*, the same set of predictors as in **Model 1** except *Substrate* and *Site*, and interactions between *Morphotype* and other predictors. To confirm that **Model 2** satisfies the assumptions of regression analysis, we inspected the residual plots. No discernible patterns were detected in the residuals.

2.4.3 Association between *Ptros*, substrate and mussel abundance

The ultimate goal of the analysis was to find out how the segregation of *ME* and *MT* between algal and bottom substrates depended on the abundance of each species on each substrate. For each site we calculated the difference between proportion of *MT* in algal and bottom samples: $Dif = P_{tros_{Algae}} - P_{tros_{Bottom}}$. The obtained *Diff* values were used as a dependent variable in **Model 3**, which was constructed as GAM with Gaussian residuals' distribution.

Assessing the dependence of *Diff* on *Ptros_{Site}*, we could not directly operate with densities of morphotypes because they were collinear on different substrates (see Results). Therefore, we performed principal component analysis for the abundance matrix of T- and E-morphotypes on algal and bottom substrates and used PC1 and PC2 values as proxies of morphotype abundances, along with *Ptros_{Site}*, in **Model 3**. As in previous cases, residual plots were examined to validate **Model 3**, and no violations of the regression analysis assumptions were detected.

2.4.4 Assessment of predictive power of Model 1

To check whether **Model 1** could be used to predict the dominant species in bottom and algal samples at a site with known environmental parameters, *MT* ($P_{tros} > 0.5$) or *ME* ($P_{tros} < 0.5$), we used all the parameters from **Model 1** to predict *Ptros_{Algae}* and *Ptros_{Bottom}* for each site within the modeling

dataset and within each of the three testing datasets. The predicted values were categorized into those greater than 0.5 and those smaller than 0.5 and considered to be classifiers for detecting *MT*- or *ME*-dominated samples. The receiver operating characteristics (ROC) followed by the analysis of the area under the curve (AUC, Fielding & Bell 1997, Fawcett 2006) were used to evaluate the performance of the models. We considered AUC greater or equal to 0.7 as acceptable discrimination (Hosmer et al., 2013). Function roc() from the package “pROC” (Robin et al. 2011) was used.

3. RESULTS

Ranges and median values of the continuous predictors are summarized in **Table 1**. While the distribution of *Fetch* and *Salinity* values was highly variable, the most wind-exposed sites were located on the southeastern coast of the Bay and on open shores of the islands in its top (**Fig. 1 A**) while the most desalinated areas were located in the very top of the Bay (**Fig. 1 C**). Expectedly, *Salinity* tended to decrease towards river mouths (**Fig. S2 A in Supplement 3**) and was lower closer to large rivers than to small ones (**Fig. S2 B in Supplement 3**). Sites close to ports tended to have lower *Fetch* (**Fig. S2 C in Supplement 3**), but no association between *DistPort* and *Salinity* was observed (**Fig. S2 D in Supplement 3**). All Pearson’s correlations between *Salinity*, *DistRiver*, *DistPort* and *Fetch* were rather low (**Table S5 in Supplement 1**), the largest being that between *Fetch* and *DistPort* ($r = 0.525$).

A striking feature visible on maps of *Ptros* distribution across algal and bottom substrates is the universally elevated proportion of *MT* on the former (**Fig. 1 D-G**). While spatial distribution of *Ptros* was highly variable, its maximum values on both substrates were observed in the Bay’s top and in some deep inlets, while its minimum values were observed along the open part of the southeastern coast (**Fig. 1 D-G**). It is difficult to discern relationships between *Ptros* and any environmental

291 predictors other than substrate in the small-scale maps shown in **Figure 1**. For this purpose, it is
292 necessary to consider **Model 1**.

293 **3.1 Relationship of *Ptros* and environmental parameters evaluated by Model 1**

294 Although some non-zero pairwise correlations between environmental factors were found (see above),
295 VIF values calculated for the predictors were generally low (maximal VIF being that for *Fetch*, 1.76).
296 This result means that the collinearity between the predictors was negligible, i.e., they did not mask
297 each other's influence.

298 **Model 1** explained 77% of the total deviance. It revealed a significant dependency of *Ptros* on all
299 predictors except *DistRiver*. Effective degrees of freedom (edf) for *DistPort* and *Fetch* were close to
300 one, indicating the linear dependence of *Ptros* on them. In contrast, the dependence on the third
301 continuous predictor, *Salinity*, was curvilinear (edf > 2, **Table 2**).

302 According to the model, *Ptros* decreased both with *DistPort* (**Fig. 2 E**) and with *Fetch* (**Fig. 2 G**). This
303 means that the proportion of *MT* was higher near ports and in surf-protected areas. *PortStatus* also had
304 a significant effect: predicted *Ptros* was higher near active ports than near abandoned ones (**Fig. 2 I**).
305 The curvilinear dependence of *Ptros* on *Salinity* can be described as follows: predicted *Ptros* decreases
306 with salinity in the range from low to about 24 psu (average salinity in the White Sea) and increases
307 again at higher salinities (up to 30 psu) (**Fig. 2 A**). In addition, predicted *Ptros* was higher near large
308 rivers than near small ones (**Fig. 2 I**). Finally, *Ptros* was higher on algal substrates than on bottom ones
309 (**Fig. 2 I**, see also **Fig 1 D-F**).

310 **3.2 Dependence of abundance of mussels of different morphotypes on environmental parameters** 311 **evaluated by Model 2**

312 The results of Model 2 were in complete good agreement with those of Model 1, the pattern of
313 association was the same for all the predictors i.e., *Salinity* (Fig. 2 B), *RiverSize* (Fig. 2 J), *DistPort*
314 (Fig. 2 F), *PortStatus* (Fig. 2 J), and *Fetch* (Fig. 2 H) (see Table S6 in Supplement 1 for all model
315 parameters). In addition, they revealed an asymmetry in the responses of the two species to some of
316 these predictors. While the abundance of T-morphotypes did not vary with *Salinity*, that of E-
317 morphotypes dropped at low salinity (Fig. 2 B). On the other hand, the abundance of E-morphotypes
318 slightly varied with *Fetch* and *DistPort*, while that of T-morphotypes strongly decreased both with the
319 distance from ports (Fig. 2 F) and with surf level (Fig. 2 H).

320 3.3 Dependency of *Ptros* on substrate and mussel abundance evaluated by Model 3

321 The principal component analysis of the abundance matrix of T- and E- morphotypes revealed a high
322 positive correlation of PC1 (explained 62% of total variation) with abundances of T-morphotypes and
323 of PC2 (20% of total variation) with abundances of E-morphotypes on both substrates (Fig. 3 B, C).
324 Thus, the abundance of conspecific morphotypes varied consistently on different substrates (see also
325 Fig. 1 D, F). Therefore, PC1 and PC2 can be considered as proxies of *MT* and *ME* abundance,
326 respectively.

327 Parameters of Model 3, which explained 31% of the deviance, are provided in ESM (Table S7 in
328 Supplement 2). Figure 3 demonstrates how the difference between *MT* proportion on algal and bottom
329 substrates (*Diff*) depends on *MT* prevalence at the site ($Ptros_{Site}$) and mussel abundances in terms of PCs
330 according to the model. The dependence of *Diff* on $Ptros_{Site}$ was significant ($p < 0.001$) and, expectedly,
331 bell-shaped, with minimal values at sites absolutely dominated by *ME* or *MT* ($Ptros$ close to 0 or 1) and
332 maximal at sites with equal presence of both species (Fig. 3 A). This means that maximum difference
333 in *Ptros* on bottom and algae substrates was observed in the settlements where the two species are

334 represented in equal proportions. This means that the strongest segregation of the two species by
335 substrate is observed in settlements where they occur in equal proportions. Dependence of *Diff* on PC1
336 was marginally significant ($p = 0.087$) and tended to decrease with increasing PC1 (**Fig. 3 B**). The
337 dependence of *Diff* on PC2 was significantly positive ($p = 0.011$, **Table S6** in **Supplement 2**, **Fig. 3 C**).
338 This means that the species were strongly segregated by substrates at sites with a high *ME* abundance,
339 which highly correlate with PC2, but not at sites with a high *MT* abundance (high correlation with
340 PC1). This means that the species were strongly segregated by substrates at sites with a high *ME*
341 abundance, but not at sites with a high *MT* abundance (remember that PC1 and PC2 are proxies for *MT*
342 and *ME* abundances respectively).

343 3.3 Assessment of predictive power of Model 1

344 **Model 1** fit well for the “Kandalaksha littoral” testing dataset (AUC=0.85 vs AUC=0.84 for modeling
345 dataset). It classified the samples into *ME*- and *MT*-dominated ones fairly well, with the exception of a
346 few false negatives, i.e., sites unpredictably dominated by *MT* (**Fig. 4 A, B**). Its predictive power for
347 the two testing sets from the Barents Sea was lower but acceptable: AUC = 0.71 for “Tyuva littoral”
348 and AUC=0.69 for “Tyuva sublittoral”. In contrast to the “Kandalaksha littoral” testing dataset, most of
349 the false results were positive.

350 4. DISCUSSION

351 Almost all environmental predictors considered in our study — namely, surf level, distance to the port,
352 status of the port, salinity at low tide, size of the nearest river and fouling substrate — influenced the
353 distribution of *Mytilus edulis* (*ME*) and *M. trossulus* (*MT*) in the White Sea. The differences in the
354 distribution reflected the partial divergence of ecological niches of these two species.

355 4.1 Ecological niche partitioning between *MT* and *ME* in the Kola contact zone

356 We showed that the most expected habitat of *ME* in the White Sea littoral was a bottom substrate in a
357 surf-exposed location with a surface salinity of 24 psu (average for the White Sea) situated away from
358 ports and large rivers. The most expected habitat of *MT* was an algal substrate in a surf-protected
359 location with a salinity lower than the White Sea average situated close to active ports and large rivers.
360 While differences associated with substrate and distance to ports have been previously noted in the
361 White Sea (Väinölä & Strelkov 2011, Katolikova et al. 2016), those associated with salinity and surf
362 exposure were first uncovered in this study.

363 4.1.1 Segregation by salinity

364 In the Baltic Sea *MT* is adapted to an extremely low salinity (Knöbel et al. 2021, Wiesenthal et al.
365 2025). Comparative experimental ecophysiological data on *MT* and *ME* elsewhere are inconclusive
366 scarce (Gardner & Thompson 2001, Qiu et al. 2002, Sokolova et al. 2024). Before our study, there has
367 been no convincing evidence of segregation of these species by salinity in contact zones outside the
368 Baltic (Moreau et al. 2005, Riginos & Cunningham 2005, Katolikova et al. 2016, Marchenko et al.
369 2023). For the White Sea, this lack of evidence could be due to at least three reasons. Firstly, the role of
370 salinity may be masked by other factors such as distance to ports. This seems particularly plausible in
371 the light of our data that *MT* in the White Sea is a euryhaline species forming mass settlements in the
372 entire salinity range recorded in our study, while *ME* is much less abundant at salinity below 15 psu
373 (**Fig. 2B**). Secondly, in contrast to the Baltic, there are no broad geographic salinity gradients in the
374 White Sea, only local ones.

375 The third reason is the curvilinear dependence of the proportion of *MT* in mixed settlements (*Ptros*) on
376 salinity: *Ptros* increases not only when the salinity is reduced but also when it is extremely high for the

377 White Sea (up to 30 psu, **Fig. 2 B**). This nonlinearity, which may prevent the dependence from being
378 detected, can be explained in two ways. On the one hand, local summer surface salinity above 24 psu in
379 the Kandalaksha Bay, supposedly associated with irregular episodes of upwelling (Dale & Prego 2003),
380 may be a nonspecific stress for littoral animals adapted to lower salinity. *MT* may be more tolerant to
381 this stress. On the other hand, as shown in detailed studies at the Barents Sea (Khaitov et al. 2021,
382 Marchenko et al. 2023), the method of predicting *Ptros* (“morphotype test”) used in our study may
383 overestimate it at salinities close to 30 psu. Therefore, we cannot rule out the possibility that the
384 increased *Ptros* at sites with a high salinity is an artifact.

385 **4.1.2 Non-random distribution depending on distance to ports**

386 The association of *MT* with harbors in the White and the Barents Sea may be associated with its
387 invasion with maritime transport from the western Atlantic in the 20th century (Väinölä & Strelkov
388 2011). It has also been hypothesized that *MT* is more resistant to anthropogenic pollution and is better
389 adapted to disturbed habitats than *ME* (Katolikova et al. 2016). Our observation that *MT* frequency is
390 lower near abandoned ports than near active ones is consistent with this hypothesis. However, the
391 propagule pressure of *MT* may have decreased near abandoned harbors in recent decades, which could
392 affect the size of its populations.

393 **4.1.3 Segregation by surf level**

394 ~~Segregation of *ME* and *MT* by surf level may be due to the well-known differences in the mechanical~~
395 ~~properties of their shells and the ability to form dense aggregations.~~ Segregation of *ME* and *MT* by surf
396 level (*ME* is more common in localities exposed to surf, while *MT* is more common in sheltered areas)
397 may be due to the well-known differences in the mechanical properties of their shells and the ability to
398 form dense aggregations. *ME* has thicker, heavier and less flexible shells (Beaumont et al. 2008,

399 Michalek et al. 2021) and is more inclined to form tight clumps (Liu et al. 2011). These features may
400 be adaptive on exposed coasts. Theoretically, the distribution of *ME* and *MT* by surf level as well as
401 substrate may also be affected by differences in byssus secretion and attachment strength.
402 Unfortunately, there are no comparative data on this topic.

403 4.1.4 Segregation by substrate

404 ~~Segregation by substrate may be explained by the same differences as segregation by surf level.~~
405 Segregation by substrate (*ME* is more common on bottom substrates, while *MT* is more common on
406 algal ones) may be explained by the same differences as segregation by surf level. Other things being
407 equal, *MT*, with its thin fragile shells, should be lighter than *ME* (Michalek et al. 2021) and thus better
408 suited to life on algae. In addition, fucoid thalli may serve as shock absorbers (Katolikova et al. 2016)
409 and provide shelter from starfish selectively preying on *MT* in mixed settlements (Khaitov et al. 2018,
410 Khaitov et al. 2023). By the same token, denser aggregations formed by *ME* are more adaptive on the
411 bottom than on algae.

412 4.1.5 Competition for substrate

413 Whatever historical, physiological, morphological, behavioral and other features influence the
414 segregation of *MT* and *ME*, interspecific competition may also be involved. Assessing the role of
415 mussel abundance in the segregation across substrates, we found that *MT* abundance did not
416 significantly affect it but *ME* abundance did: as the latter increased, the degree of segregation
417 increased, too (**Fig. 3 B, C**). In our opinion, this pattern results from the divergence of the realized, but
418 not fundamental, species niches: *ME* outcompetes *MT* on bottom substrates displacing it to algal thalli.

419 Spatial segregation of sympatric mussels by substrates, which is apparently density-dependent, is
420 evident at the level of tens of centimeters (Katolikova et al. 2016). Direct analogies for segregation at

such a small scale can be found in other attached organisms, terrestrial plants (Raventós et al. 2010). A biologically generated spatial pattern model (Pacala & Levin 1997, Amarasekare 2003) relates inter-specific segregation with the intra-specific clustering in competing species. Our findings suggest that this model can also be applied to mussels.

4.2 Predictive power of SDM

The ability of our model to classify sites into *ME*- and *MT*-dominated ones in an independent testing dataset from the White Sea was high (AUC = 0.85). Therefore, we assume that the predictors included in the model explain most of the variation in species distribution within the littoral fucoid belt in the White Sea.

~~The worst, though formally satisfactory predictive value of the model for the Barents Sea data (AUC ≈ 0.7) may be due to the following reasons.~~ The model's predictive performance for the Barents Sea data (AUC ≈ 0.7), while formally acceptable, was lower than for the White Sea. This may be due to the following reasons. Firstly, it may be associated with a large depth range of the sampling sites, considering that distribution of *ME* and *MT* in the Tyuva Inlet by depth is non-random (Marchenko et al. 2023). The second reason may be a coarser categorization of the Barents Sea samples into algal and bottom ones. Since fouling substrate was not taken into account during sampling, we predicted it based on the projective cover of algae at the sampling site. Thirdly, we do not know whether the two species are non-randomly distributed across bottom and algal substrates in the sublittoral, where fucoids are replaced by kelps. The fourth reason could be a narrow variation in the values of *DistPort*, *DistRiver*, and *Fetch* in the small Tyuva Inlet in comparison with the Kandalaksha Bay.

Finally, the fact that SDM tended to overestimate *Ptros* in the Barents Sea data (false positive predictions) is consistent with the observation that the proportion of *MT* has been declining in the study

area in the 2010s under seemingly stable environmental conditions in terms of predictors included in our model (Marchenko et al. 2023). This observation suggests the presence of some yet unstudied factors regulating the taxonomic structure.

4.3 Ecological niche partitioning between MT and ME in the Kola contact zone as compared to other zones

Blue mussels are a challenging model for studying ecological niche partitioning between cryptic species in sympatry due to their wide distribution, biogeographic history and hybridization. *ME* and *MT* play similar ecological roles in their native oceans, Atlantic and Pacific, respectively (compare Comito & Dankers 2001 and Bodkin et al. 2018) and may inherently have overlapping fundamental ecological niches. Contact zones between these species in the Atlantic can be considered as ecological (and evolutionary) experiments, set in strikingly different environments (from Baltic to Spitsbergen) at different times (from late post-glacial to the historical period, Väinölä & Strelkov 2011, Wenne et al. 2020, and references therein). The design of these experiments was possibly different too, because in some zones the original settler could be *ME* and in others, *MT*. In addition, competition (ecological character displacement, Pfennig & Pfennig 2009), hybridization (reinforcement of prezygotic reproductive isolation, Lukhtanov 2011) and introgression (adaptive introgression, Hedrick 2013) could influence the divergence of their ecological phenotypes differently in different zones. These considerations suggest that the zones should differ, and this hypothesis has been a recurrent theme in genetic research on blue mussel contact zones (Riginos & Cunningham 2005, Bierne et al. 2011, Fraïsse et al. 2016). Nevertheless, we believe that the differences between *ME* and *MT* are more fundamental and that conspecific ecological phenotypes in different zones should thus be similar,

464 producing comparable patterns in species distributions. Some results of this study support this
465 hypothesis.

466 The observation that *MT* frequency is elevated in low-salinity habitats not only in the Baltic but also in
467 the White Sea seems to resolve the old conundrum about seemingly contrasting salinity adaptations of
468 the Baltic and other Atlantic *MT* populations (e.g. Riginos & Cunningham 2005, Katolikova et al.
469 2016, see also above). Further, an increased *MT* frequency has been repeatedly observed in calm and
470 freshened waters e.g., in the tops of fjords near Bergen in Norway (Ridgway & Nævdal 2004) and
471 Uummannaq in Greenland (Wenne et al. 2020) and in Loch Etive in Scotland (Beaumont et al. 2008),
472 which is hardly a coincidence. Our observations indicate that this combination of weak surf and low
473 salinity is also favorable for *MT* in the White Sea.

474 With the exception of salinity in the Baltic, none of the predictors affecting segregation of *ME* and *MT*
475 in the White Sea have been convincingly shown to act in other contact zones. Data on surf are
476 inconsistent (compare Bates & Innes 1995, Comesaña et al. 1999, Tam & Scrosati 2014 and this study),
477 and data on substrates are absent. If different preferences of *ME* and *MT* for surf level and substrates
478 are indeed associated with their morphological and behavioral differences (Katolikova et al. 2016; this
479 study), these preferences should be omnipresent. Ad hoc studies in other contact zones might throw
480 light on this matter. It would also be interesting to examine the differences between *ME* and *MT* in
481 tolerance to stress, particularly anthropogenic pollution, e.g., in harbors (see discussion in Brooks et al.
482 2015 and Beyer et al. 2017).

483 **4.4 Strengths and weaknesses of our approaches to the study of sympatric mussels**

484 The methods used in our study have certain limitations. We identified the mussels with the help of the
485 “morphotype test”, which does not permit a direct assessment of species abundances and does not

486 identify hybrids as a separate category. The latter limitation is not particularly significant in the Kola
487 zone, where hybrids are relatively scarce (Väinölä & Strelkov 2011, Wenne et al. 2020), but may
488 compromise studies in other contact zones, where hybrids may play an important ecological role (e.g.,
489 Schwartz et al. 2024).

490 Although *ME* and *MT* differ everywhere in morphotype frequencies, the magnitude of the differences
491 varies between contact zones and between habitats with different salinities in the Arctic (Khaitov et al.
492 2021). This means that the “morphotype test” must be calibrated before use in a new area (see Khaitov
493 et al. 2021 for recommendations). Multilocus genotyping, while still too costly for processing dozens
494 of thousands of specimens needed for SDM, remains the gold standard of taxonomic assessment in blue
495 mussels.

496 We did not account for some potential predictors affecting species segregation such as depth
497 (Marchenko et al. 2023), predators (Khaitov et al. 2018, Khaitov et al. 2023) or temperature (Kijewski
498 et al. 2019). Moreover, some of our predictors could have been estimated more carefully (for example,
499 bottom salinity at high tide could be more informative for littoral mussels than salinity at low tide).
500 However, since most of our predictors were shown to be significant, they should not be ignored in
501 future studies.

502 The correlative approach used in our study does not allow a direct assessment of either relative or
503 absolute importance of factors. For instance, we cannot say whether salinity or substrate is more
504 crucial. However, the take-home message from our research is that there is no single “leading” factor
505 determining the distribution of *ME* and *MT*, contrary to the idea that has dominated the field since the
506 pioneering studies in the Baltic (e.g. Gardner & Thompson 2001, Ridgway & Nævdal 2004, Riginos &
507 Cunningham 2005, Śmietanka et al. 2014).

508 The limitations discussed above do not detract from the fact that, as shown in our study, SDMs may be
509 a useful tool for the study of distribution of *ME* and *MT* in sympatry. Their obvious benefits include the
510 possibility to analyze the distribution of the species in the space of multiple predictors simultaneously,
511 the possibility to control the collinearity of the predictors and the lack of necessity to treat
512 dependencies as linear.

513 Promising directions of further research on niche partitioning in sympatric mussel species are, ~~in our~~
514 ~~opinion,~~ as follows. The use of taxonomic methods allowing direct assessment of abundances of
515 species and their hybrids would elucidate the nature of competition between them all. Incorporation of
516 additional environmental factors into SDMs might yield surprising results. Further, it would be
517 worthwhile to have a closer look at different spatial scales, down to the smallest one, in the segregation
518 of these two mussel species. Finally, a parallel study in different contact zones would reveal common
519 and zone-specific patterns. The classical review on the divergence of ecological niches of *ME* and *MT*
520 in different contact zones (Riginos & Cunningham 2005) is 20 years old. The time is ripe for a new
521 survey, and our observations from the Kola zone may prove useful.

522 *ACKNOWLEDGEMENTS*

523 We thank all participants of our expeditions, especially Gita Paskerova and Eugene Genelt-Yanovsky,
524 for their help in fieldwork. We are deeply grateful to Natalia Lentsman for the English language
525 assistance during the preparation of the manuscript. We would like to express our special gratitude to
526 the administration of the Kandalaksha State Nature Reserve, where a significant part of the material
527 was collected, for comprehensive assistance. We also thank three anonymous reviewers for their
528 constructive feedback that substantially improved the paper. This study was supported by the Russian
529 Science Foundation, grant no. 19-74-20024.

530 *LITERATURE CITED*

- 531 Amarasekare P (2003) Competitive coexistence in spatially structured environments: A synthesis.
532 Ecology Letters 6:1109–1122.
- 533 Austin MP (2002) Spatial prediction of species distribution: an interface between ecological theory and
534 statistical modelling. Ecological modelling 157:101–118.
- 535 Bates J, Innes D (1995) Genetic variation among populations of *Mytilus* spp. in eastern Newfoundland.
536 Marine Biology 124:417–424.
- 537 Beaumont AR, Hawkins MP, Doig FL, Davies IM, Snow M (2008) Three species of *Mytilus* and their
538 hybrids identified in a Scottish Loch: natives, relicts and invaders? Journal of Experimental Marine
539 Biology and Ecology 367:100–110.
- 540 Berger V, Dahle S, Galaktionov K, Kosobokova X, Naumov A, Rat'kova T, Savinov V, Savinova T
541 (2001) White Sea. Ecology and Environment. St-Petersburg-Tromso: Derzavets Publishers.
- 542 Berger VY, Naumov A (2000) General features of the White Sea. Berichte Polarf 359:3–9.
- 543 Beyer J, Green NW, Brooks S, Allan IJ, Ruus A, Gomes T, Bråte ILN, Schøyen M (2017) Blue
544 mussels (*Mytilus edulis* spp.) as sentinel organisms in coastal pollution monitoring: A review. Marine
545 Environmental Research 130:338–365.
- 546 Bickford D, Lohman DJ, Sodhi NS, Ng PKL, Meier R, Winker K, Ingram KK, Das I (2007) Cryptic
547 species as a window on diversity and conservation. Trends in Ecology and Evolution 22:148–155.
- 548 Bierne N, Welch J, Loire E, Bonhomme F, David P (2011) The coupling hypothesis: why genome
549 scans may fail to map local adaptation genes. Molecular ecology 20:2044–2072.
- 550 Bjornstad ON (2022) ncf: Spatial Covariance Functions. R package version 1.3-2.

551 Bjørnstad ON, Falck W (2001) Nonparametric spatial covariance functions: Estimation and testing.
 552 Environmental and Ecological Statistics 8:53–70.

553 Bodkin JL, Coletti HA, Ballachey BE, Monson DH, Esler D, Dean TA (2018) Variation in abundance
 554 of Pacific blue mussel (*Mytilus trossulus*) in the Northern Gulf of Alaska, 2006–2015. Deep Sea
 555 Research Part II: Topical Studies in Oceanography 147:87–97.

556 Brooks SJ, Farmen E, Heier LS, Blanco-Rayón E, Izagirre U (2015) Differences in copper
 557 bioaccumulation and biological responses in three *Mytilus* species. Aquatic Toxicology 160:1–12.

558 Buschbaum C, Dittmann S, Hong JS, Hwang IS, Strasser M, Thiel M, Valdivia N, Yoon SP, Reise K
 559 (2009) Mytilid mussels: Global habitat engineers in coastal sediments. Helgoland Marine Research
 560 63:47–58.

561 Caradima B, Schuwirth N, Reichert P (2019). From individual to joint species distribution models: A
 562 comparison of model complexity and predictive performance. Journal of Biogeography 46:2260–2274.

563 Comesaña AS, Toro JE, Innes DJ, Thompson RJ (1999) A molecular approach to the ecology of a
 564 mussel (*Mytilus edulis* - *M. trossulus*) hybrid zone on the east coast of Newfoundland, Canada. Marine
 565 Biology 133:213–221.

566 Commito JA, Dankers NM (2001) Dynamics of spatial and temporal complexity in european and north
 567 american soft-bottom mussel beds. In: *Ecological comparisons of sedimentary shores*. Springer, p 39–
 568 59

569 Dale AW, Prego R (2003) Tidal and seasonal nutrient dynamics and budget of the Chupa Estuary,
 570 White Sea (Russia). Estuarine, Coastal and Shelf Science 56:377–389.

571 Dennis AB, Hellberg ME (2010) Ecological partitioning among parapatric cryptic species. Molecular
572 Ecology 19:3206–3225.

573 Druehl LD, Green JM (1982) Vertical distribution of intertidal seaweeds as related to patterns of
574 submersion and emersion. Marine Ecology Progress Series 9:163–170.

575 Dufresnes C, Poyarkov N, Jablonski D (2023) Acknowledging more biodiversity without more species.
576 Proceedings of the national Academy of Sciences 120:e2302424120.

577 Elith J, H. Graham C, P. Anderson R, Dudík M, Ferrier S, Guisan A, J. Hijmans R, Huettmann F, R.
578 Leathwick J, Lehmann A, Li J, G. Lohmann L, A. Loiselle B, Manion G, Moritz C, Nakamura M,
579 Nakazawa Y, McC. M. Overton J, Townsend Peterson A, J. Phillips S, Richardson K, Scachetti-Pereira
580 R, E. Schapire R, Soberón J, Williams S, S. Wisz M, E. Zimmermann N (2006) Novel methods
581 improve prediction of species' distributions from occurrence data. Ecography 29:129–151.

582 Elith J, Leathwick JR (2009) Species Distribution Models: Ecological Explanation and Prediction
583 Across Space and Time. Annual review of ecology, evolution, and systematics 40:677–697.

584 Fawcett T (2006) An introduction to ROC analysis. Pattern Recognition Letters 27:861–874.

585 Fielding AH, Bell JF (1997) A Review of Methods for the Assessment of Prediction Errors in
586 Conservation Presence/Absence Models. Environmental conservation 24:38–49.

587 Filatov N, Pozdnyakov D, Johannessen OM, Pettersson LH, Bobylev LP (2007) White Sea: its marine
588 environment and ecosystem dynamics influenced by global change. Springer Science & Business
589 Media.

590 Fox J, Monette G (1992) Generalized collinearity diagnostics. Journal of the American Statistical
591 Association 87:178–183.

592 Fraïsse C, Belkhir K, Welch JJ, Bierne N (2016) Local interspecies introgression is the main cause of
593 extreme levels of intraspecific differentiation in mussels. *Molecular Ecology* 25:269–286.

594 Gardner JPA, Thompson RJ (2001) The effects of coastal and estuarine conditions on the physiology
595 and survivorship of the mussels *Mytilus edulis*, *M. trossulus* and their hybrids. *Journal of Experimental*
596 *Marine Biology and Ecology* 265:119–140.

597 Gardner JP, Oyarzun PA, Toro JE, Wenne R, Zbawicka M (2021) Phylogeography of Southern
598 Hemisphere blue mussels of the genus *Mytilus*: evolution, biosecurity, aquaculture and food labelling.
599 In: *Oceanography and marine biology*. CRC Press, p 139–228

600 Geller JB, Darling JA, Carlton JT (2010) Genetic perspectives on marine biological invasions. *Annual*
601 *review of marine science* 2:367–393.

602 Gosling E (2021) *Marine mussels: ecology, physiology, genetics and culture*. John Wiley & Sons.

603 Hayhurst S, Rawson PD (2009) Species-specific variation in larval survival and patterns of distribution
604 for the blue mussels *Mytilus edulis* and *Mytilus trossulus* in the Gulf of Maine. *Journal of Molluscan*
605 *Studies* 75:215–222.

606 Hedrick PW (2013) Adaptive Introgression in Animals: Examples and Comparison to New Mutation
607 and Standing Variation as Sources of Adaptive Variation. *Molecular ecology* 22:4606–4618.

608 Hellou J, Law RJ (2003) Stress on stress response of wild mussels, *Mytilus edulis* and *Mytilus*
609 *trossulus*, as an indicator of ecosystem health. *Environmental Pollution* 126:407–416.

610 Hosmer JrDW, Lemeshow S, Sturdivant RX (2013) *Applied logistic regression*. John Wiley & Sons.

611 Hu Z-M, Zhang Q-S, Zhang J, Kass JM, Mammola S, Fresia P, Draisma SG, Assis J, Jueterbock A,
 612 Yokota M, Zhang Z (2021) Intraspecific genetic variation matters when predicting seagrass distribution
 613 under climate change. *Molecular Ecology* 30:3840–3855.

614 Katolikova M, Khaitov V, Väinölä R, Gantsevich M, Strelkov P (2016) Genetic, ecological and
 615 morphological distinctness of the blue mussels *Mytilus trossulus* Gould and *M. edulis* L. in the White
 616 Sea. *PLoS One* 11:e0152963.

617 Khaitov V, Makarycheva A, Gantsevich M, Lentsman N, Skazina M, Gagarina A, Katolikova M,
 618 Strelkov P (2018) Discriminating eaters: Sea stars *Asterias rubens* L. feed preferably on *Mytilus*
 619 *trossulus* Gould in mixed stocks of *Mytilus trossulus* and *Mytilus edulis* L. *Biological Bulletin* 234:85–
 620 95.

621 Khaitov V, Marchenko J, Katolikova M, Väinölä R, Kingston SE, Carlon DB, Gantsevich M, Strelkov
 622 P (2021) Species identification based on a semi-diagnostic marker: Evaluation of a simple
 623 conchological test for distinguishing blue mussels *Mytilus edulis* L. and *M. trossulus* Gould. *PLoS*
 624 *ONE* 16:1–27.

625 Khaitov VM, Makarycheva AY, Nematova RB, Evdokimova AI (2023) Predators regulate the
 626 taxonomic structure of mixed *Mytilus edulis* L. and *M. trossulus* Gould settlements in the shallow
 627 waters of the White Sea. *Proceedings of the Zoological Institute of the Russian Academy of Sciences*
 628 327:8–24.

629 Kijewski T, Zbawicka M, Strand J, Kautsky H, Kotta J, Rätsep M, Wenne R (2019) Random forest
 630 assessment of correlation between environmental factors and genetic differentiation of populations:
 631 Case of marine mussels *Mytilus* . *Oceanologia* 61:131–142.

632 Knöbel L, Nascimento-Schulze JC, Sanders T, Zeus D, Hiebenthal C, Barboza FR, Stuckas H, Melzner
 633 F (2021) Salinity Driven Selection and Local Adaptation in Baltic Sea Mytilid Mussels. *Frontiers in*
 634 *Marine Science* 8:692078.

635 Knowlton N (1993) Sibling Species in the Sea. *Annual review of ecology and systematics* 24:189–216.

636 Koehn RK (1991) The genetics and taxonomy of species in the genus *Mytilus* . *Aquaculture* 94:125–
 637 145.

638 Krasavtsev LB (2011) Russia’s foreign trade through the ports of the White Sea in the early twentieth
 639 century. (in Russian). *Vestnik Severnogo (Arkticheskogo) federal’nogo universiteta Seriya:*
 640 *Gumanitarnye i social’nye nauki* 1:17–24.

641 Lindegren M, Gabellini AP, Munk P, Edelvang K, Hansen FT (2022) Identifying key processes and
 642 drivers affecting the presence of non-indigenous marine species in coastal waters. *Biological Invasions*
 643 24:2835–2850.

644 Liu G, Stapleton E, Innes D, Thompson R (2011) Aggregational behavior of the blue mussels *Mytilus*
 645 *edulis* and *Mytilus trossulus*: A potential pre-zygotic reproductive isolation mechanism. *Marine*
 646 *Ecology* 32:480–487.

647 Lowen JB, Hart DR, Stanley RRE, Lehnert SJ, Bradbury IR, Dibacco C, Hauser L (2019) Assessing
 648 effects of genetic, environmental, and biotic gradients in species distribution modelling. *ICES Journal*
 649 *of Marine Science* 76:1762–1775.

650 Lukhtanov V (2011) Dobzhansky’s rule and reinforcement of prezygotic reproductive isolation in
 651 zones of secondary contact. *Biology Bulletin Reviews* 1:2–12.

652 Marchand P, Gill D (2018) waver: Calculate Fetch and Wave Energy. R package version 0.2.1.

653 Marchenko J, Khaitov V, Katolikova M, Sabirov M, Malavenda S, Gantsevich M, Basova L, Genelt-
 654 Yanovsky E, Strelkov P (2023) Patterns of spatial and temporal dynamics of mixed *Mytilus edulis* and
 655 *M. trossulus* populations in a small subarctic inlet (Tyuva Inlet, Barents Sea). *Frontiers in Marine*
 656 *Science* 10:1–15.

657 Michalek K, Vendrami DLJ, Bekaert M, Green DH, Last KS, Telesca L, Wilding TA, Hoffman JI
 658 (2021) *Mytilus trossulus* introgression and consequences for shell traits in longline cultivated mussels.
 659 *Evolutionary Applications* 14:1830–1843.

660 Morais P, Reichard M (2018) Cryptic invasions: A review. *Science of the Total Environment*
 661 613:1438-1448.

662 Moreau V, Tremblay R, Bourget E (2005) Distribution of *Mytilus edulis* and *M. trossulus* on the Gaspé
 663 coast in relation to spatial scale. *Journal of Shellfish Research* 24:545–551.

664 Ovaskainen O, Abrego N (2020) *Joint Distribution Modelling (with applications in R).* Cambridge
 665 University Press.

666 Pacala SW, Levin SA (1997) Biologically generated spatial pattern and the coexistence of competing
 667 species. In: *Spatial ecology: The role of space in population dynamics and interspecific interactions.*
 668 *Monographs in Population Biology.* Princeton University Press Princeton, NJ, p 204–232

669 Penney RW, Hart MJ, Templeman N (2002) Comparative growth of cultured blue mussels, *Mytilus*
 670 *edulis*, *M. trossulus* and their hybrids, in naturally occurring mixed-species stocks. *Aquaculture*
 671 *Research* 33:693–702.

672 Peterson ML, Doak DF, Morris WF (2019) Incorporating local adaptation into forecasts of species'
 673 distribution and abundance under climate change. *Global Change Biology* 25:775–793.

674 Pfennig K, Pfennig D (2009) Character displacement: ecological and reproductive responses to a
675 common evolutionary problem. *The Quarterly Review of Biology* 84:253–276.

676 Poggiato G, Münkemüller T, Bystrova D, Arbel J, Clark JS, Thuiller W (2021). On the interpretations
677 of joint modeling in community ecology. *Trends in ecology & evolution* 36:391-401.

678 Qiu JW, Tremblay R, Bourget E (2002) Ontogenetic changes in hyposaline tolerance in the mussels
679 *Mytilus edulis* and *M. trossulus*: Implications for distribution. *Marine Ecology Progress Series*
680 228:143–152.

681 Quinn GP, Keough MJ (2002) Experimental design and data analysis for biologists. Cambridge
682 university press.

683 R Core Team (2023) R: A Language and Environment for Statistical Computing. R Foundation for
684 Statistical Computing, Vienna, Austria.

685 Raventós J, Wiegand T, Luis MD (2010) Evidence for the spatial segregation hypothesis: a test with
686 nine-year survivorship data in a Mediterranean shrubland. *Ecology* 91:2110–2120.

687 Reiss H, Cunze H, König K, Neumann K, Kröncke I (2011) Species distribution modelling of marine
688 benthos: A North Sea case study. *Marine Ecology Progress Series* 442:71–86.

689 Ridgway G, Nævdal G (2004) Genotypes of *Mytilus* from waters of different salinity around Bergen,
690 Norway. *Helgoland Marine Research* 58:104–109.

691 Riginos C, Cunningham CW (2005) Local adaptation and species segregation in two mussel (*Mytilus*
692 *edulis* x *Mytilus trossulus*) hybrid zones. *Molecular Ecology* 14:381–400.

693 Robin X, Turck N, Hainard A, Tiberti N, Lisacek F, Sanchez J-C, Müller M (2011) pROC: an open-
694 source package for R and S+ to analyze and compare ROC curves. *BMC Bioinformatics* 12:77.

695 Sáez AG, Lozano E (2005) Body doubles. *Nature* 433:111-111.

696 Sailing directions of the White Sea (1932) Leningrad : izdanie i tipografiya Gidrograficheskogo
697 upravleniya. (in Russian).

698 Schwartz LC, González VL, Strong EE, Truebano M, Hilbish TJ (2024) Transgressive gene expression
699 and expression plasticity under thermal stress in a stable hybrid zone. *Molecular Ecology* 33:e17333.

700 Simon A, Fraïsse C, El Ayari T, Liautard-Haag C, Strelkov P, Welch JJ, Bierne N (2021) How do
701 species barriers decay? Concordance and local introgression in mosaic hybrid zones of mussels. *Journal*
702 *of Evolutionary Biology* 34:208–223.

703 Śmietanka B, Burzyński A, Hummel H, Wenne R (2014) Glacial history of the European marine
704 mussels *Mytilus*, inferred from distribution of mitochondrial DNA lineages. *Heredity* 113:250–258.

705 Sokolova IM, Kovalev A, Timm S, Marchenko J, Sukhotin A (2024) Species-specific metabolome
706 changes during salinity downshift in sub-Arctic populations of *Mytilus edulis* and *M. trossulus* .
707 *Frontiers in Marine Science* 11:1403774.

708 Struck TH, Feder JL, Bendiksbj M, Birkeland S, Cerca J, Gusarov VI, Kistenich S, Larsson K-H, Liow
709 LH, Nowak MD, others (2018) Finding evolutionary processes hidden in cryptic species. *Trends in*
710 *Ecology & Evolution* 33:153–163.

711 Stuckas H, Knöbel L, Schade H, Breusing C, Hinrichsen HH, Bartel M, Langguth K, Melzner F (2017)
712 Combining hydrodynamic modelling with genetics: can passive larval drift shape the genetic structure
713 of Baltic *Mytilus* populations? *Molecular Ecology* 26:2765–2782.

714 Tam JC, Scrosati RA (2014) Distribution of cryptic mussel species (*Mytilus edulis* and *M. trossulus*)
715 along wave exposure gradients on northwest Atlantic rocky shores. Marine Biology Research 10:51–
716 60.

717 Väinölä R, Strelkov P (2011) *Mytilus trossulus* in northern Europe. Marine Biology 158:817–833.

718 Wenne R, Zbawicka M, Bach L, Strelkov P, Gantsevich M, Kukliński P, Kijewski T, McDonald JH,
719 Sundaasen KK, Árnýasi M, Lien S, Kaasik A, Herkül K, Kotta J (2020) Trans-atlantic distribution and
720 introgression as inferred from single nucleotide polymorphism: mussels *Mytilus* and environmental
721 factors. Genes 11:530.

722 Wiesenthal AA., Timm S, Sokolova IM (2025) Osmotolerance reflected in mitochondrial respiration of
723 *Mytilus* populations from three different habitat salinities. Marine Environmental Research, 205:
724 106968.

725 Wood SN (2017) Generalized additive models: An introduction with R. Chapman; hall/CRC.

726 Zbawicka M, Sańko T, Strand J, Wenne R (2014) New SNP markers reveal largely concordant clinal
727 variation across the hybrid zone between *Mytilus* spp. in the Baltic Sea. Aquatic Biology 21:25–36.

728 Zolotarev V, Shurova N (1997) Relations of prismatic and nacreous layers in the shells of the mussel
729 *Mytilus trossulus*. Russian Journal of Marine Biology 23:26–31.

730

731 Table 1. Environmental parameters involved in the study

Environmental parameter/ model predictor	Type	Explanation	Range (median) in the data
<i>Influence of substrate</i>			
<i>Substrate</i>	Categorical	Algal and Bottom samples for each site are treated separately.	Algae VS Bottom
<i>Influence of rivers</i>			
<i>Salinity</i>	Continuous	Surface salinity (psu) at the time of sampling, i.e. at low tide.	2-30 (19)
<i>DistRiver</i>	Continuous	The straight line distance (km) between the site and the nearest river mouth by map. The values were log-transformed when used for model fitting.	0-18.5 (4.9)
<i>RiverSize</i>	Categorical	Rivers are categorized according to whether their catchment area is larger or smaller than the median area of all rivers in the region.	Small VS Large
<i>Influence of ports</i>			
<i>DistPort</i>	Continuous	The straight line distance (km) between the site and the nearest port by map. Log-transformed values were used.	0.1-82.2 (18.7)
<i>PortStatus</i>	Categorical	Ports are categorized according to whether they are active or abandoned.	Active VS Abandoned
<i>Influence of surf</i>			
<i>Fetch</i>	Continuous	Unobstructed length of water surface (km) over which wind from a certain direction can blow. Log-transformed values were used.	0.2-28.8 (3.3)

732

71

36

72

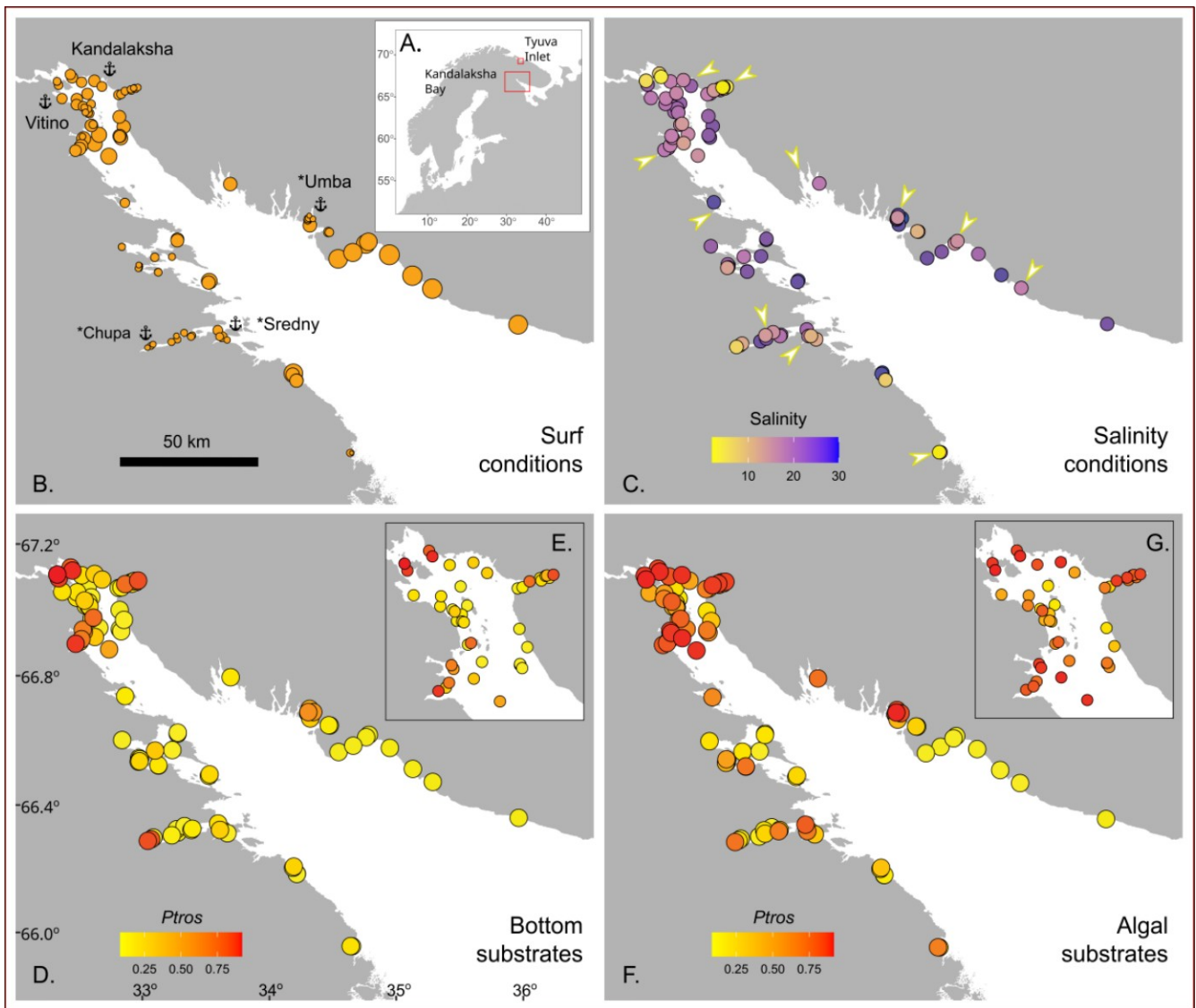
733

734 Table 2. Parameters of smoothers and coefficients of parametric terms for Model 1 describing
 735 dependency of proportion of *Mytilus trossulus* in mixed settlements (*Ptros*) on environmental
 736 predictors. **Smoother's summary**: edf – effective degrees of freedom; ref.edf – reference effective
 737 degrees of freedom.

738

Smoother terms	edf	ref.edf	Chi square	p-value
<i>s(Salinity)</i>	2.4	9	396.7	0.003
<i>s(DistRiver)</i>	0.0	9	0.0	0.672
<i>s(Fetch)</i>	0.9	9	88.2	0.042
<i>s(DistPort)</i>	1.0	9	276.2	0.002
Random effect <i>s(Site)</i>	74.4	92	453.6	<0.0001
Parametric terms	Parameter estimate	SE	z-statistic	p-value
(Intercept)	-1.7	0.1	-11.8	<0.0001
Substrate _(Algae)	0.9	0.1	14.6	<0.0001
RiverSize _(Large)	0.4	0.2	2.6	0.009
PortStatus _(Active)	1.0	0.2	5.7	<0.0001

739



740

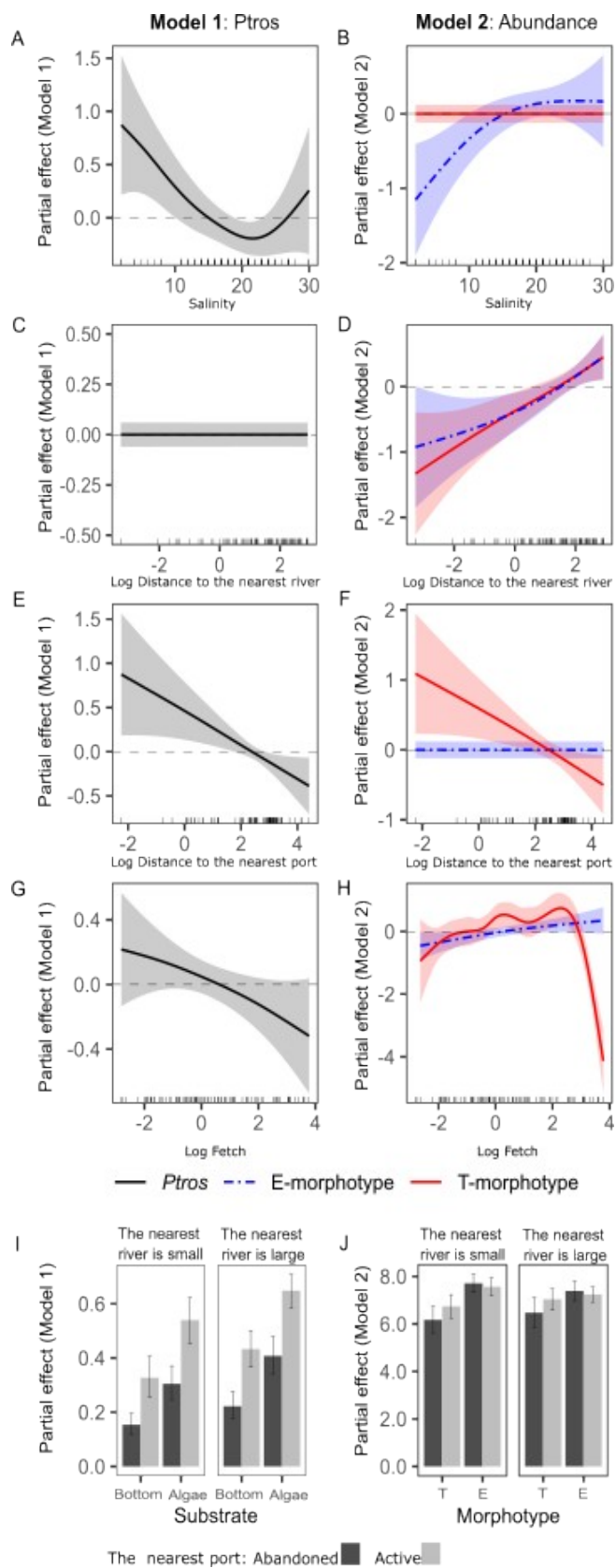
741

742 **Figure 1.** Taxonomic structure of mussel settlements and their habitat characteristics. (A) Map of
 743 Northern Europe. Red boxes mark the position of Kandalaksha Bay and Tyuva Inlet. Maps on B-G
 744 represent the Kandalaksha Bay. Land is shown in gray, sea is shown in white. (B) Surf conditions.
 745 Point size is proportional to *Fetch*. Anchors with names mark ports. Asterisks identify whether the port
 746 is currently abandoned. (C) Salinity conditions. Point filling is proportional to *Salinity*. Arrows mark
 747 mouths of large rivers. (D-G) Proportion of *Mytilus trossulus* in bottom (*Ptros_{Bottom}*, D-E) and algal

75

76

748 ($Ptros_{Algae}$, F-G) samples. Point filling is proportional to $Ptros$. E and G show the Bay's top in higher
749 resolution.



750

79

80

40

751 Figure 2. Partial effects of environmental parameters on either proportion of *Mytilus trossulus* in mixed
752 settlements (*Ptros*) or abundance of species-specific morphotypes evaluated by GAM(M)s fitted
753 (**Model 1** and **Model 2**, respectively). Dependency of *Ptros* on salinity at low tide (*Salinity*, **A**),
754 distance to the nearest river (*DistRiver*, **C**), distance to the nearest port (*DistPort*, **E**), wind exposure
755 (*Fetch*, **G**), and discrete predictors: substrate type, nearest port status and size of the nearest river (**I**).
756 Dependency of E- and T-morphotype *log-transformed* abundances on *Salinity* (**B**), *DistRiver* (**D**),
757 *DistPort* (**F**), *Fetch* (**H**), and nearest port status and size of the nearest river (**J**). Ribbons around curves
758 and whiskers represent 95% confidence intervals.

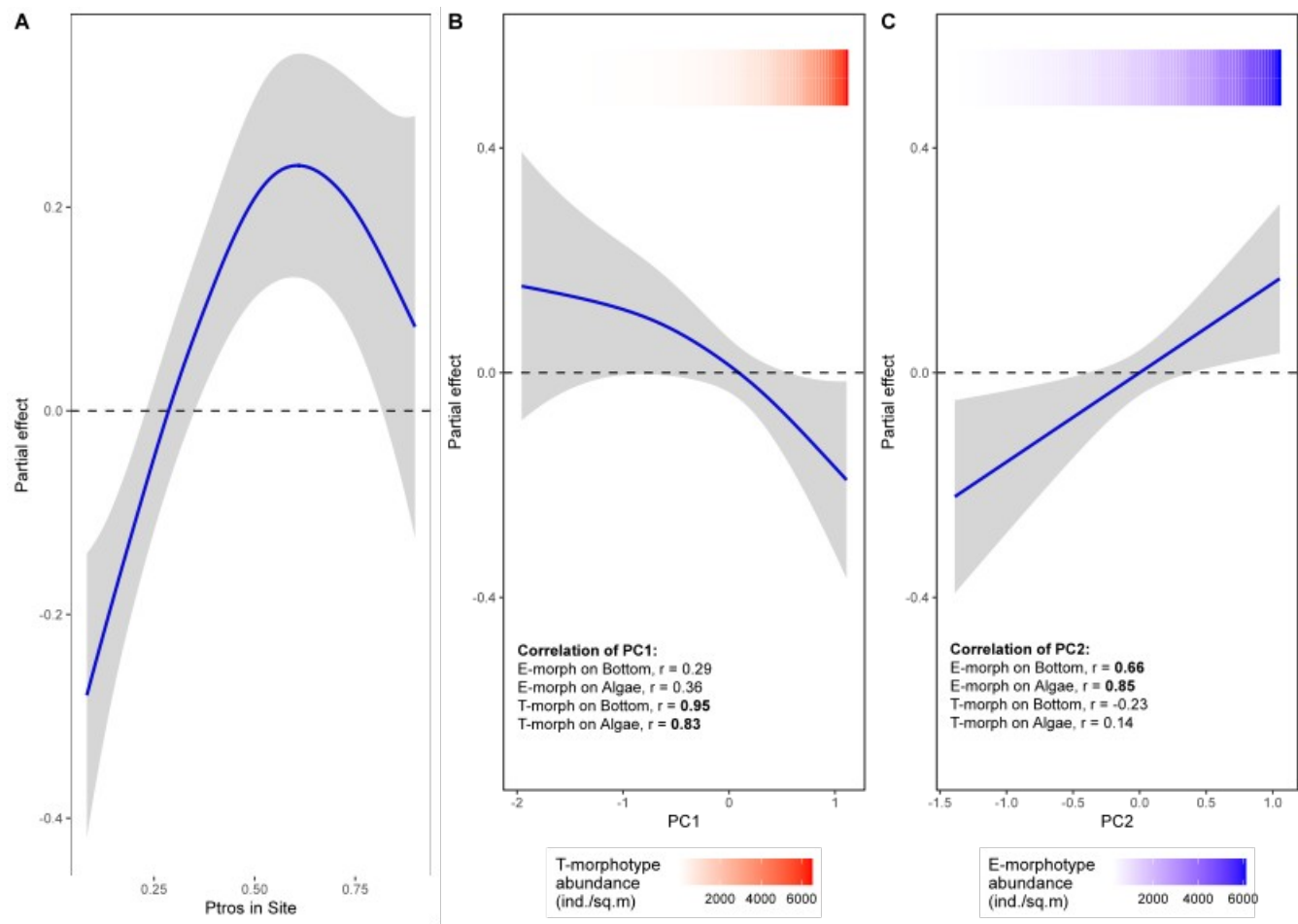
760

761

762 **Figure 3.** The dependence of difference between proportion of *Mytilus trossulus* on algal and
763 bottom substrates (*Diff*) on proportion of *M. trossulus* in a site (*Ptros_{Site}*) (A) and estimations of
764 total abundance of *M. trossulus* (B) and *Mytilus edulis* (C). Principal components from the
765 matrix of T- and E-morphotypes abundances on different substrates are considered as proxies for
766 *M. trossulus* and *M. edulis* abundances (PC1 and PC2, respectively). Correlations of mussel
767 abundances with PC scores are given, two highest coefficients are given in bold. Ribbons around

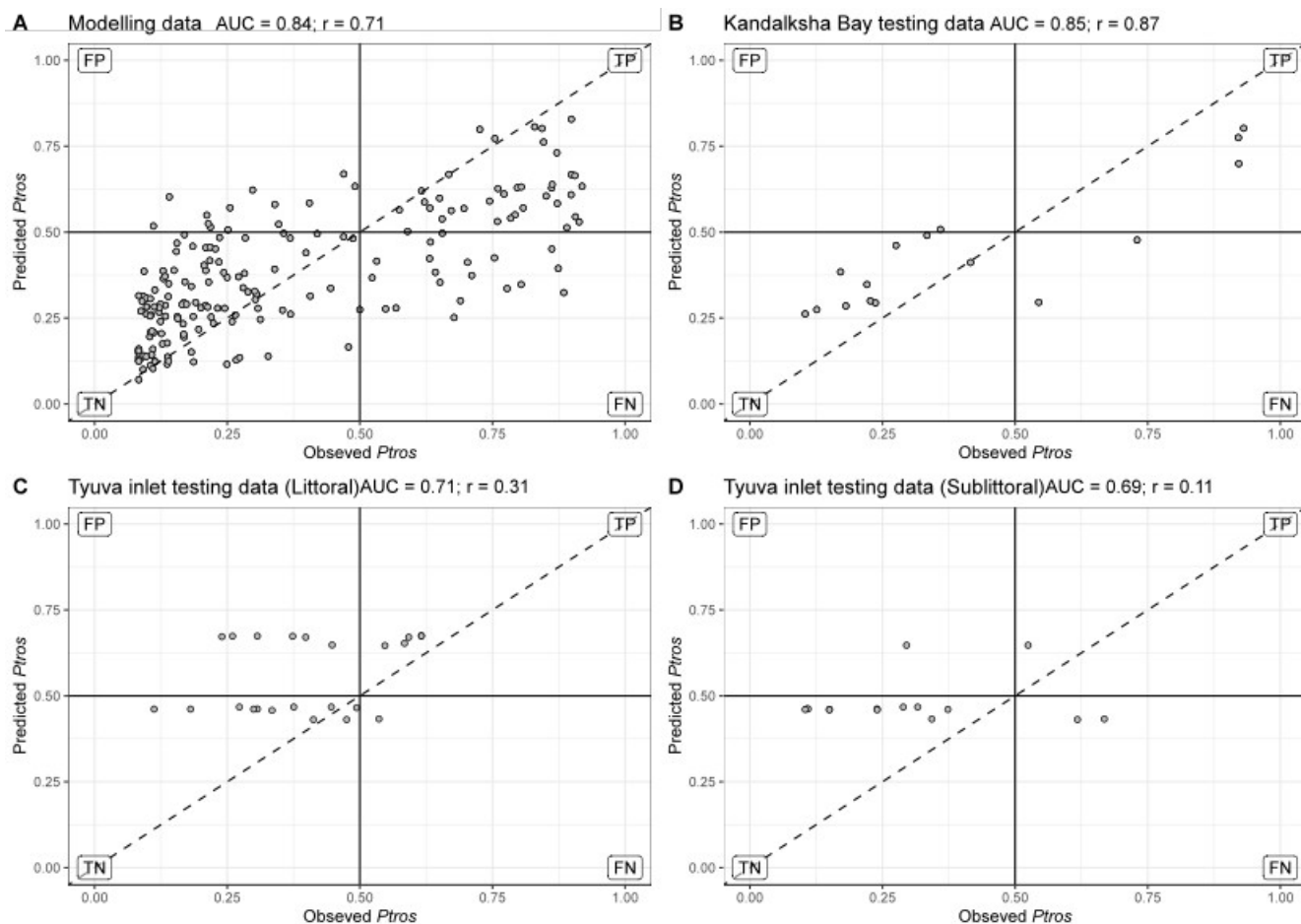
83

84



768 curves represent 95% confidence intervals. Colored gradient bars at the top of the figures reflect linear
769 associations between PC1 and T-morphotype (B) and PC2 and E-morphotype abundance (C).

770



771

772

773 **Figure 4.** Ability of SDM (**Model 1**) to predict proportion of *MT Mytilus trossulus* (*Ptros*) in mussel
 774 samples from the modeling (A) and the testing datasets (B-D). Each plot compares empirical *Ptros* in
 775 samples from algal and bottom substrates and *Ptros* predicted by the model within the particular
 776 dataset. If the empirical and the predicted values were the same, the points would lie on the diagonal
 777 (dashed line). Labels mark the quadrants with false positive (FP), true positive (TP), true negative (TN)
 778 and false negative (FN) predictions in the analysis of the ability of the model to classify samples into
 779 *ME Mytilus edulis*-dominated ($Ptros < 0.5$) and *MT M. trossulus*-dominated ($Ptros > 0.5$) ones. Dataset

87

88

780 names are shown in chart headers. Values of AUC for binary classification (~~ME-dominated~~ vs ~~MT-~~
781 ~~dominated~~ *M. edulis*-dominated vs *M. trossulus*-dominated) and Pearson correlations between observed
782 and predicted *Ptros* are given in figure headings.

783